Propagation of Bragg-Reflected Neutrons in Bounded Mosaic Crystals

S. A. WERNER AND ANTHONY ARROTT
Scientific Laboratory, Ford Motor Company, Dearborn, Michigan

AND

J. S. KING AND H. KENDRICK
Department of Nuclear Engineering, University of Michigan, Ann Arbor, Michigan

(Received 29 November 1965)

The analysis of the multiple Bragg reflection of a neutron beam of finite size in a semi-infinite mosaic crystal given in a recent paper by Werner and Arrott is generalized to include bounded crystals. The coupled differential equations describing secondary extinction given by Hamilton are solved in general, and a method of piecewise solution, or solution by regions, is given.

A discussion is given of experiments on the spatial distribution of the diffracted current from slab-shaped crystals. Various methods for measuring the probability for Bragg scattering per unit path are compared and found not to agree. It is felt that the discrepancies are basic to the mosaic structure of crystals in general.

I. INTRODUCTION

IN a recent paper[1] the multiple Bragg-scattering problem in a semi-infinite mosaic crystal was discussed in considerable detail. The starting point of the analysis was a pair of coupled, integral equations describing the incident and diffracted current densities. In this paper the coupled, differential equations given by Hamilton[2] are solved in general, and a method of piecewise solution, or solution by regions, is given for crystals of finite size.

A thermal neutron beam may penetrate quite deeply into a mosaic crystal before it is diffracted and subsequently multiply diffracted; consequently, the results of a neutron diffraction experiment represent a sampling of the bulk material in contrast to x-ray and electron diffraction experiments where surface preparation is of prime importance due to absorption in the first case and the strength of the interaction in the latter. It is felt that full advantage of this fact has not been taken particularly by metallurgists studying dislocations and mosaic structure. However, in order to use neutron diffraction as a tool in studying single-crystal growth and mosaic structure, a reasonably complete understanding of the multiple-Bragg reflection (or secondary extinction) of neutrons in crystals of finite size is necessary. It is essential that the problems treated are realistic in the sense that both the incident beam and the crystal are of finite size.

In addition to the motivation for this study provided by the above discussion and the historic interest in being able to correct for secondary extinction in the determination of crystallographic structures, we have been interested in the theory of monochromation of neutrons in an effort to make better use of the thermal neutron beams available at low-to-medium-flux reactors. Consequently, the problems treated in Sec. II are the diffraction of neutrons in slab crystals oriented in the Bragg and Laue positions.[3] It is pointed out that rectangular-shaped crystals provide no additional difficulty. A brief discussion of some rather extensive experiments on the multiple-Bragg reflection of neutrons and mosaic structure is given in Sec. III.

II. MULTIPLE REFLECTION IN A CRYSTAL OF THICKNESS T

A. Bragg Case

This section is devoted to finding the incident and diffracted current densities, denoted by $J_i(x,s)$ and $J_D(x,s)$, respectively, in and on the boundaries of a mosaic crystal cut in the form of a slab of thickness T. (x,s) is a point in the nonorthogonal coordinate system shown in Fig. 1. The reciprocal lattice vector of interest makes an angle β with the normal to the crystal surface such that the reflecting planes are not necessarily parallel to the surface. We let the beam incident on the crystal be finite in width and constant between $y_0=0$ and $y_0=W_0$ (and zero elsewhere), where y_0 is a coordinate orthogonal to the incident wave vector $\mathbf{k}$ as

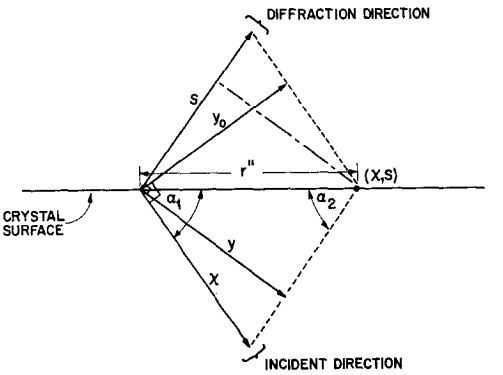

FIG. 1. Coordinate systems used in the analysis. **x** and **s** are directions of the incident and diffracted beams, respectively. $\mathbf{y}_0$ is perpendicular to **x**, **y** is perpendicular to **s**.

[1] S. A. Werner and A. Arrott, Phys. Rev. **140**, A675 (1965). This paper will be referred to as BRI.
[2] W. C. Hamilton, Acta Cryst. **10**, 629 (1957).
[3] See, for example, W. H. Zachariasen, *X-Ray Diffraction in Crystals* (John Wiley & Sons, Inc., New York, 1944), p. 120.

shown in Fig. 1. This "plane source" assumption is, of course, not necessary, but the calculation closely approximates real experimental situations for neutrons of a given **k** emerging from a rectangular collimator. The results of this paper can be integrated (numerically) over **k** to include the angular and momentum divergence of the incident beam.

It is apparent from the work reported in BRI[1] that the diffracted current density on the entrant surface of the crystal will consist of two parts, and can be found from the solution of the problem of a semi-infinite incident beam. The solution for a finite beam is the difference of the solution for a semi-infinite beam with origin at $y_0=0$ and the solution for the semi-infinite beam with origin displaced by the fraction β_2/β_1 of the width of the incident finite beam. Thus, if $J_D(y)$ is the diffracted current density along the surface for the finite beam, and $N_D(y)$ is the solution for the semi-infinite beam, then

$$J_D(y)=N_D(y)-N_D[y-(\beta_2/\beta_1)W_0] \times u_{-1}[y-(\beta_2/\beta_1)W_0]. \quad (1)$$

$N_D(y)$ is the diffracted current density on the surface expressed as a distribution function in the coordinate y measured perpendicular to the diffracted wave vector resulting from a semi-infinite incident beam (i.e., $W_0\rightarrow\infty$), and u_{-1} is the unit step function. β_1 and β_2 are the sines of the two angles $(\theta_B+\beta)$ and $(\theta_B-\beta)$, respectively, where θ_B is the Bragg angle. We therefore solve the problem in which a semi-infinite beam impinges on the crystal as shown in Fig. 2. The solution for the diffracted current density on the surface as a result of an incident beam of finite width is found by subtracting two displaced $N_D(y)$ curves according to Eq. (1).

The balance relations for the conservation of neutrons entering and leaving the infinitesimal parallelogram shown in Fig. 3 are[4]

$$\partial J_i/\partial x=-\Sigma_t J_i+\Sigma_s J_D \quad (2)$$

and

$$\partial J_D/\partial s=-\Sigma_t J_D+\Sigma_s J_i, \quad (3)$$

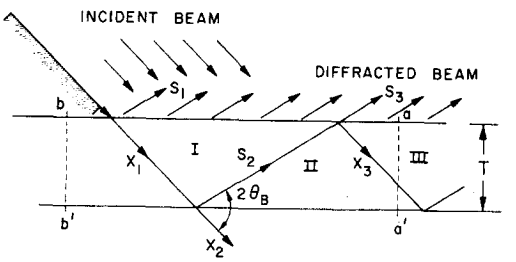

FIG. 2. Geometry of a semi-infinite beam impinging on a crystal of finite thickness T. The planes dividing regions I, II, III, etc. are loci of points where the current densities have at least one discontinuous derivative. The coordinate system for each region is indicated by the vectors $\mathbf{x}_n$ and $\mathbf{s}_n$.

[4] These equations were given by Hamilton (1957).

where $\Sigma_s(\mathbf{k})$ is defined to be the probability per unit path, for small paths, that a neutron having wave vector **k** will be Bragg reflected.[5] Similarly $\Sigma_t(\mathbf{k})$ is defined to be the probability per unit path for small paths that a neutron having wave vector **k** suffers any interaction which changes its course (including absorption). We assume as a first-order approximation that Σ_s and Σ_t are spatially invariant. Combining Eqs. (2) and (3) yields the following elliptical equation:

$$\partial^2 J_D/\partial x\partial s+\Sigma_t\partial J_D/\partial x+\Sigma_t\partial J_D/\partial s +(\Sigma_t^2-\Sigma_s^2)J_D=0. \quad (4)$$

A similar equation holds for $J_i(x,s)$. For the present problem of a semi-infinite incident beam, $J_i(x,s)$ and $J_D(x,s)$ in the above equations are replaced by $N_i(x,s)$ and $N_D(x,s)$. The boundary conditions are

$$N_i \text{ (entrant surface)}=1 \quad \text{for} \quad y_0\geq 0 \quad (5)$$

and

$$N_D \text{ (back surface)}=0. \quad (6)$$

The solution to this problem does not have continuous derivatives throughout the entire crystal. The discontinuity in the beam incident on the crystal along the line $s_1=0$, coupled with the discontinuities in Σ_s and Σ_t at the two surfaces of the crystal, give rise to discontinuities in the derivatives of $N_D(x,s)$ and $N_i(x,s)$ along certain lines. In this section we demonstrate that separate solutions with continuous derivatives exist in each of the regions labelled I, II, III, etc. in Fig. 2.

The method of solution consists of solving the problem for each region separately. The solution in the $(n-1)$th region will be used as a boundary condition for the solution in the nth region. The current densities in the nth region are labeled $N_D^n(x_n,s_n)$ and $N_i^n(x_n,s_n)$, where the coordinates (x_n,s_n) are shown in Fig. 2.

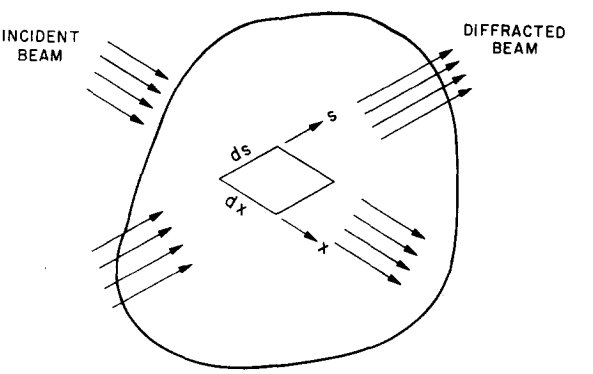

FIG. 3. Parallelogram, of sides dx and ds, on which the balance relations (2) and (3) are based.

[5] It is apparent that $\Sigma_s(\mathbf{k})=\Sigma_s(\mathbf{k}+2\pi\mathbf{G})$, where **G** is the reciprocal lattice vector of interest. Commonly used expressions for Σ_s are given in Ref. 1.

Region I

The boundary conditions for the current densities in region I are

$$N_i^{\mathrm{I}}[x_1,(\beta_1/\beta_2)x_1]=1 \text{ (entrant surface)}, \; x_1>0 \quad (7)$$

and

$$N_i^{\mathrm{I}}(x_1,0)=\exp(-\Sigma_t x_1). \quad (8)$$

We look for a solution of Eq. (4) of the form

$$N_D^{\mathrm{I}}(x_1,s_1)=\exp[-\Sigma_t(x_1+s_1)]f_D^{\mathrm{I}}(x_1,s_1). \quad (9)$$

Substitution of this expression into (4) gives

$$[\partial^2 f_D^{\mathrm{I}}(x_1,s_1)/\partial x_1\partial s_1]-\Sigma_s^2 f_D^{\mathrm{I}}(x_1,s_1)=0. \quad (10)$$

The general solution of this equation is

$$f_D^{\mathrm{I}}(x_1,s_1)=\int A^{\mathrm{I}}(K)\exp\left[K\Sigma_s x_1+\frac{1}{K}\Sigma_s s_1\right]dK, \quad (11)$$

where the contour of integration in the K plane is not specified at this point. The function $A^{\mathrm{I}}(K)$ is to be determined by the boundary conditions. Since N_D^{I} and N_i^{I} satisfy differential equations of the same form, we must also have,

$$N_i^{\mathrm{I}}(x_1,s_1)=\exp[-\Sigma_t(x_1+s_1)]\times\int B^{\mathrm{I}}(K)\exp\left(K\Sigma_s x_1+\frac{1}{K}\Sigma_s s_1\right)dK. \quad (12)$$

Using Eq. (3) we find that

$$B^{\mathrm{I}}(K)=A^{\mathrm{I}}(K)/K. \quad (13)$$

Writing f_D^{I} as

$$f_D^{\mathrm{I}}(x_1,s_1)=\int A^{\mathrm{I}}(K)\times\exp\left\{\Sigma_s(x_1s_1)^{\frac{1}{2}}\left[K\left(\frac{x_1}{s_1}\right)^{\frac{1}{2}}+\frac{1}{K}\left(\frac{s_1}{x_1}\right)^{\frac{1}{2}}\right]\right\}dK, \quad (14)$$

and using the expansion

$$\exp[y(\mu+1/\mu)]=\sum_{n=-\infty}^{\infty}\mu^n I_n(2y), \quad (15)$$

(where I_n is a modified Bessel function of the first kind of order n) we have

$$f_D^{\mathrm{I}}(x_1,s_1)=\sum_{n=-\infty}^{\infty}a_n^{\mathrm{I}}\left(\frac{x_1}{s_1}\right)^{n/2}I_n[2\Sigma_s(x_1s_1)^{\frac{1}{2}}], \quad (16)$$

where

$$a_n^{\mathrm{I}}\equiv\int K^n A(K)dK. \quad (17)$$

From Eq. (13), the solution for f_i^{I} is then

$$f_i^{\mathrm{I}}\equiv\exp[\Sigma_t(x_1+s_1)]N_i(x_1,s_1)=\sum_{n=-\infty}^{\infty}a_{n-1}^{\mathrm{I}}\left(\frac{x_1}{s_1}\right)^{n/2}I_n[2\Sigma_s(x_1s_1)^{\frac{1}{2}}]. \quad (18a)$$

Applying the boundary conditions [Eqs. (7) and (8)] we find,

$$\left\{\begin{array}{l}a_n^{\mathrm{I}}=0, \quad \text{for} \quad n\geq 0\\ a_{-1}^{\mathrm{I}}=1\\ a_{-n}^{\mathrm{I}}=(\beta_2/\beta_1)^{(n-1)/2}[c_0{}^{n-1}+c_0{}^{-n+1}]\end{array}\right\}, \quad (18b)$$

where

$$c_0=c_1+(c_1{}^2-1)^{\frac{1}{2}},$$

and

$$c_1=\tfrac{1}{2}(\Sigma_t/\Sigma_s)[(\beta_1/\beta_2)^{\frac{1}{2}}+(\beta_2/\beta_1)^{\frac{1}{2}}].$$

Since $I_n=I_{-n}$, we write N_D^{I} as

$$N_D^{\mathrm{I}}(x_1,s_1)=\exp[-\Sigma_t(x_1+s_1)]\left\{\left(\frac{s_1}{x_1}\right)^{\frac{1}{2}}I_1[2\Sigma_s(x_1s_1)^{\frac{1}{2}}]+\sum_{n=2}^{\infty}\left(\frac{\beta_2}{\beta_1}\right)^{(n-1)/2}(c_0{}^{n-1}+c_0{}^{-n+1})\left(\frac{s_1}{x_1}\right)^{n/2}I_n[2\Sigma_s(x_1s_1)^{\frac{1}{2}}]\right\}. \quad (18c)$$

When this solution is evaluated along the surface of the crystal, we have the same result as given by Eqs. (39a) and (39b) of BRI. That is, the solution in region I is the same as for the semi-infinite crystal.

Region II

In order to solve the problem in region II the x coordinate is shifted by an amount T/β_1 as shown in Fig. 2. The differential equation (4) applies also to N_D^{II} with a similar equation for N_i^{II}. Thus, the solution must again be of the same form as equation (9), that is

$$N_D^{\mathrm{II}}(x_2,s_2)=\exp[-\Sigma_t(x_2+s_2-T/\beta_1)]f_D^{\mathrm{II}}(x_2,s_2)$$

and (19)

$$N_i^{\mathrm{II}}(x_2,s_2)=\exp[-\Sigma_t(x_2+s_2-T/\beta_1)]f_i^{\mathrm{II}}(x_2,s_2),$$

where the constant $\exp(\Sigma_t T/\beta_1)$ is factored out of f_i^{II} and f_D^{II} so that the boundary conditions can be applied more easily on the interface between regions I and II. The equations for f_D^{II} and f_i^{II} are of the form of Eq. (10), so

$$f_D^{\mathrm{II}}(x_2,s_2)=\int A^{\mathrm{II}}(K)\exp\left(K\Sigma_s x_2+\frac{1}{K}\Sigma_s s_2\right)dK \quad (20)$$

$$f_i^{\mathrm{II}}(x_2,s_2)=\int A^{\mathrm{II}}(K)/K\exp\left(K\Sigma_s x_2+\frac{1}{K}\Sigma_s s_2\right)dK. \quad (21)$$

The boundary conditions on these solutions are

$$f_D^{\mathrm{II}}\text{ (back surface)}=0, \quad (22)$$

while on the interface between regions I and II

$$f_D^{\mathrm{I}}(\text{interface})=f_D^{\mathrm{II}}(\text{interface}),$$
$$\text{and} \tag{23}$$
$$f_i^{\mathrm{I}}(\text{interface})=f_i^{\mathrm{II}}(\text{interface}).$$

Defining

$$a_n^{\mathrm{II}}=\int A^{\mathrm{II}}(K)K^n dK, \tag{24}$$

and applying the above boundary conditions, we get

$$\left\{\begin{array}{l} a_{-l}^{\mathrm{II}}=\sum_{m=0}^{\infty}\left[\dfrac{(\Sigma_s T/\beta_1)^m}{m!}\right]a_{m-l}^{\mathrm{I}} \quad \text{for} \quad l\geq 1 \\ a_0^{\mathrm{II}}=0 \\ a_l^{\mathrm{II}}=-(\beta_1/\beta_2)^l a_{-l}^{\mathrm{II}} \quad \text{for} \quad l\geq 1. \end{array}\right\} \tag{25}$$

Since all a_n^{I} are known and are given by Eqs. (18b), we can calculate all a_n^{II}. Thus the solutions in region II are now known:

$$N_i^{\mathrm{II}}(x_2,s_2)=\exp[-\Sigma_t(x_2+s_2-T/\beta_1)] \times\sum_{n=-\infty}^{\infty} a_{n-1}^{\mathrm{II}}\left(\frac{x_2}{s_2}\right)^{n/2} I_n[2\Sigma_s(x_2 s_2)^{\frac{1}{2}}] \tag{26}$$

$$N_D^{\mathrm{II}}(x_2,s_2)=\exp[-\Sigma_t(x_2+s_2-T/\beta_1)] \times\sum_{n=-\infty}^{\infty} a_n^{\mathrm{II}}\left(\frac{x_2}{s_2}\right)^{n/2} I_n[2\Sigma_s(x_2 s_2)^{\frac{1}{2}}]. \tag{27}$$

We proceed in the same manner to obtain the solution in region III from the solution in region II, and finally the solution in the nth region in terms of the coefficients in the $(n-1)$th region. The equations for calculating all a_m^n are given in the Appendix. Using these regions we can obtain numerical values for N_i and N_D at all points in the crystal. The general solutions for the nth region are

Odd regions: $n=2l+1$

$$N_i^n(x_n,s_n) =\exp\left[-\Sigma_t\left(x_n+s_n-\frac{n-1}{2}\frac{T}{\beta_1}-\frac{n-1}{2}\frac{T}{\beta_2}\right)\right]f_i^n(x_n,s_n)$$
$$N_D^N(x_n,s_n) =\exp\left[-\Sigma_t\left(x_n+s_n-\frac{n-1}{2}\frac{T}{\beta_1}-\frac{n-1}{2}\frac{T}{\beta_2}\right)\right]f_D^n(x_n,s_n). \tag{28}$$

Even regions: $n=2l$

$$N_i^n(x_n,s_n) =\exp\left[-\Sigma_t\left(x_n+s_n-\frac{n}{2}\frac{T}{\beta_1}-\frac{n}{2}\frac{T}{\beta_2}\right)\right]f_i^n(x_n,s_n)$$
$$N_D^n(x_n,s_n) =\exp\left[-\Sigma_t\left(x_n+s_n-\frac{n}{2}\frac{T}{\beta_1}-\frac{n}{2}\frac{T}{\beta_2}\right)\right]f_D^n(x_n,s_n), \tag{29}$$

where

$$f_i^n(x_n,s_n)=\sum_{m=-\infty}^{\infty} a_{m-1}^n\left(\frac{x_n}{s_n}\right)^{m/2} I_m[2\Sigma_s(x_n s_n)^{\frac{1}{2}}]$$
$$f_D^n(x_n,s_n)=\sum_{m=-\infty}^{\infty} a_m^n\left(\frac{x_n}{s_n}\right)^{m/2} I_m[2\Sigma_s(x_n s_n)^{\frac{1}{2}}]. \tag{30}$$

[The actual functional dependence of $A^{\mathrm{I}}(K)$, $A^{\mathrm{II}}(K)$, etc. on K can be established if the contour of integration is taken as a circle about the origin in the K plane. Expanding $A^n(K)$ in a Laurent series about the origin,

$$A^n(K)=\sum_{l=-\infty}^{\infty} b_l^n K^l,$$

one obtains

$$b_{-l}^n=\frac{1}{2\pi i}\oint\frac{A^n(K)}{K^{l+1}}dK,$$

according to Laurent's theorem. But

$$\oint K^{-l-1}A^n(K)dK\equiv a_{-l-1}^n,$$

so

$$A^n(K)=\frac{1}{2\pi i}\sum_{l=-\infty}^{\infty} a_{l-1}^n K^l,$$

where all a_{l-1}^n are known.]

These solutions for the problem of the slab of finite thickness give results which are of the same general form as for the infinitely thick slab. The diffracted beam leaving the crystal surface in region I is identical to that for the infinitely thick slab. A deviation begins with a discontinuity in the derivatives of $N_D(y)$ on passing from region I to region III (see Fig. 4). For large distances from the origin (where the incoming beam starts), $N_D(y)$ reaches the asymptotic value for the finite crystal. For the symmetric case ($\beta_1/\beta_2=1$) and no absorption ($\Sigma_t/\Sigma_s=1$), the asymptotic value (found by applying the same total current equations of BRI) depends on crystal thickness according to

$$N_D(\text{asymptotic})=[1+(\beta_1/\Sigma_s T)]^{-1}. \tag{31}$$

This is plotted as the upper curve in Fig. 5. This result may be compared with the intensity at the end of the first region.

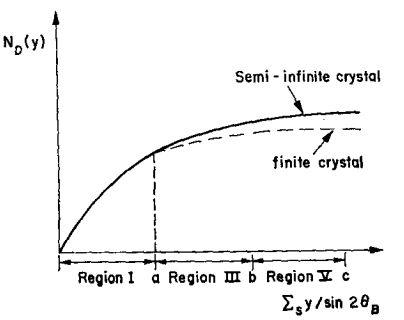

FIG. 4. Comparison of $N_D(y)$ for a finite crystal with $N_D(y)$ for a semi-infinite crystal.

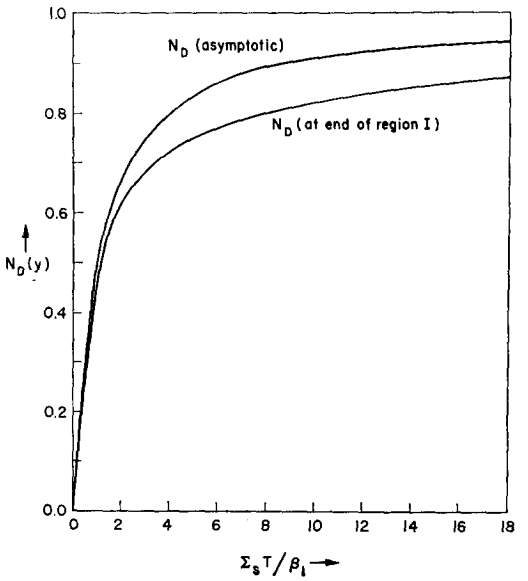

FIG. 5. Comparison of $N_D(y)$ at the end of the first region and its asymptotic value as a function of crystal thickness.

We note that, for very thin crystals, N_D (end of region I) is very near the asymptotic value. At thicknesses corresponding to $\Sigma_s T/\beta_1 \approx 8.0$ the difference reaches a maximum of about 10% of the asymptotic value. As the thickness T increases still further, the difference between the diffracted current density at the end of the first region and its asymptotic value slowly falls off, ultimately to zero when the crystal becomes infinitely thick. Consequently, if one calculates the asymptotic value of $N_D(y)$ and uses Figs. 11(a)–11(e) of BRI (which apply for the semi-infinite crystal), the part of the curve for $N_D(y)$ corresponding to regions III, V, etc. on the surface of the crystal can be sketched in easily (Fig. 4). As a result, the exact solutions, Eqs. (28), (29), and (30), need be used only if very accurate plots of $N_D(y)$ are required, e.g., to obtain the tails on the $J_D(y)$ vs y curves.

It should be noted that cutting the infinite lateral slab off along a plane such as $a-a'$ (see Fig. 2) does not alter the solutions obtained in this section. Cutting the crystal off along the plane $b-b'$ (thereby forming a rectangular crystal) would simply add an additional part to the solution due to current entering the crystal through the boundary plane $b-b'$. This part of the solution is easily obtained using the methods of this section. Consequently, the secondary extinction coefficients for rectangular crystals [as obtained by Hamilton by numerical integration of Eqs. (2) and (3)] can be calculated.

B. Laue Case, Delta-Function Beam

We now inquire about the multiple reflection of a pencil beam entering a slab crystal at a point A as shown in Fig. 6. The equations to be solved are again (2) and (3). The boundary condition on ${}_\delta J_D(x,s)$ are

$$ {}_\delta J_D(0,s) = \Sigma_s \exp(-\Sigma_t s) \tag{32}$$

and

$$ {}_\delta J_D(x,0) = \Sigma_s \exp(-\Sigma_t x), \tag{33}$$

where the subscript δ refers to a delta-function beam. For a solution of the form

$$ \delta J_D(x,s) = \exp[-\Sigma_t(x+s)] \times \int A(K) \exp(K\Sigma_s x + \Sigma_s s/K) dK, \tag{34}$$

$$ \Sigma_s = \int A(K) \exp(K\Sigma_s s) dK, \tag{35}$$

and

$$ \Sigma_s = \int A(K) \exp(\Sigma_s x/K) dK \tag{36}$$

or

$$ a_n \equiv \int K^n A(K) dK = \begin{cases} \Sigma_s & \text{for } n=0 \\ 0 & \text{for } n \neq 0 \end{cases}. \tag{37}$$

Consequently, after expansion of the integral in (34) in a series of Bessel functions as done in Eq. (6), ${}_\delta J_D(x,s)$ assumes the simple form

$$ {}_\delta J_D(x,s) = \Sigma_s \exp[-\Sigma_t(x+s)] I_0[2\Sigma_s(xs)^{\frac{1}{2}}]. \tag{38}$$

The current density ${}_\delta J_i(x,s)$ can be found in a similar manner. It is

$$ {}_\delta J_i(x,s) = \delta(s) \exp(-\Sigma_t x) + \exp[-\Sigma_t(x+s)] \times \Sigma_s (x/s)^{\frac{1}{2}} I_1[2\Sigma_s(xs)^{\frac{1}{2}}]. \tag{39}$$

The diffracted current density on the back surface of the crystal between the points B and C is shown in Fig. 7 for various crystal thicknesses T (for the special case where $\beta_1=\beta_2$ and $\Sigma_t=\Sigma_s$). These profiles are relatively flat as is physically apparent from the fact that the total path length $(x+s)$ from the point A to any point on the back surface between B and C is a constant.

C. Laue Case, Distributed Beam

We now consider the problem where a crystal is used in the transmission position and the incident beam is

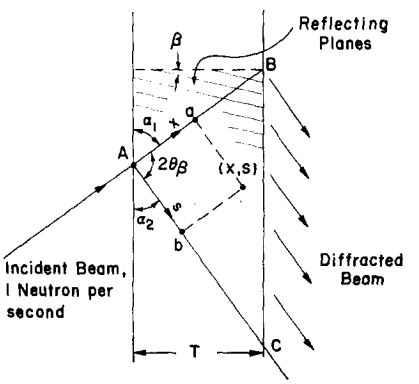

FIG. 6. Diffraction of a delta-function beam in a mosaic crystal placed in the Laue position.

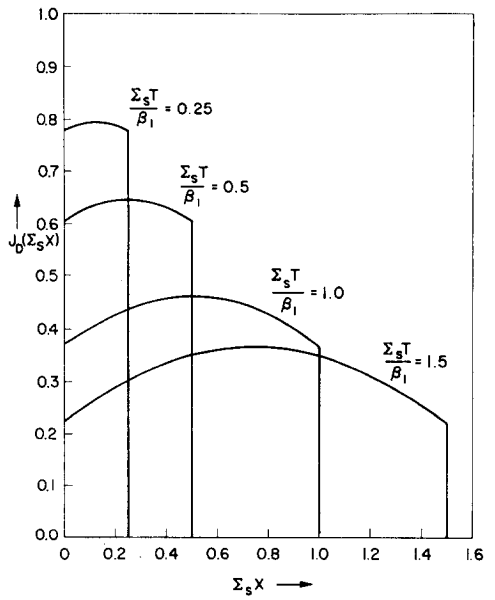

FIG. 7. Curves showing the diffracted current density on the surface BC of Fig. 6 for various values of the dimensionless parameter $\Sigma_s T/\beta_1$. $\beta_1=\beta_2$ and $\Sigma_t=\Sigma_s$ for the curves plotted.

distributed over a width W_0 as shown in Fig. 8. The solution for ${}_\delta J_D$ from the last paragraph could be used as a Green's function for this problem. However, the solution can be more easily obtained by treating it as a two-region, boundary-value problem.

The current densities are nonzero in the region bounded by ABCDEA. The width W of the diffracted beam can be considerably larger than the width of the incident beam W_0. The incident beam is again assumed to be constant from point A to point E (and zero elsewhere). The diffracted current density J_D on the back surface of the crystal due to a beam of finite width can again

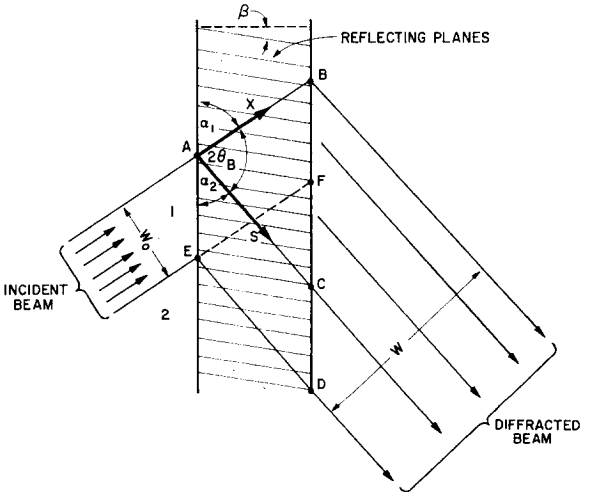

FIG. 8. Laue case: the incident beam is distributed over the width W_0. The angles are related by $\alpha_1=\pi/2-\theta_B-\beta$, and $\alpha_2=\pi/2-\theta_B+\beta$. J_D and J_i are nonzero only in the region bounded by ABCDEA.

be calculated by subtracting two N_D curves. That is,

$$J_D=N_D(\mathrm{B})-N_D(\mathrm{F}). \tag{40}$$

$N_D(\mathrm{B})$ is the same function as $N_D(\mathrm{F})$ displaced by an amount BF. $N_D(\mathrm{B})$ is the diffracted current density due to a semi-infinite incident beam which starts at point A; and $N_D(\mathrm{F})$ is the diffracted current density due to a semi-infinite beam which starts at point E. Consequently, we need only solve the semi-infinite beam problem. This problem consists of two regions as shown in Figs. 9(a) and 9(b) due to the discontinuity in the derivative of $N_D(x,s)$ along the line AC.

Region I. All points (x,s) along the line a'-a in region I are equivalent; consequently, the current densi-

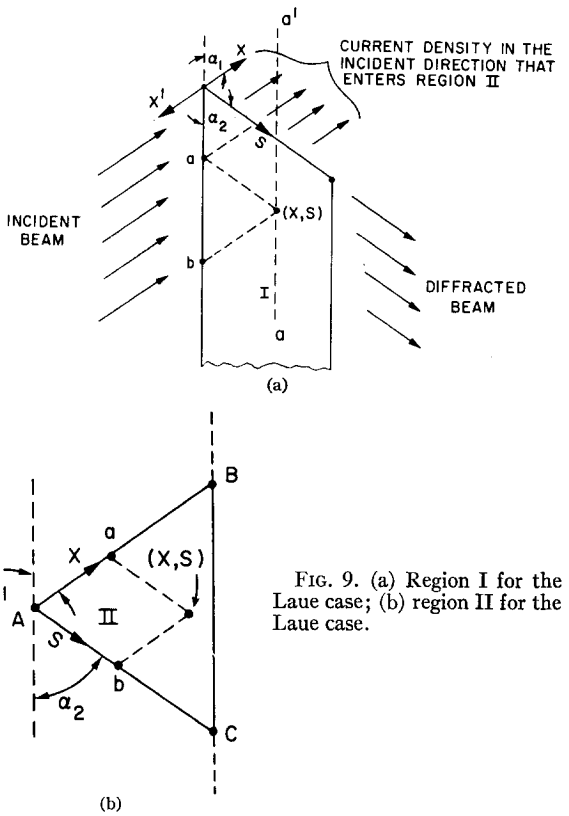

FIG. 9. (a) Region I for the Laue case; (b) region II for the Laue case.

ties can be written as a function of one variable h which is the distance from the entrant surface to the line a'-a. This distance is

$$h=\beta_2 s+\beta_1 x, \tag{41}$$

$$\text{where } \beta_2\equiv\sin\alpha_2, \quad \beta_1\equiv\sin\alpha_1.$$

A solution for the diffracted current density which satisfies the boundary conditions $N_D{}^{\mathrm{I}}=0$ and $N_i{}^{\mathrm{I}}=1$ along the entrant surface is

$$N_D{}^{\mathrm{I}}(x,s)=[\Sigma_s/\beta_2(D_1-D_2)] \times[\exp(D_1 h)-\exp(D_2 h)]. \tag{42}$$

The incident current density can be calculated from

Eq. (3) as

$$N_i^{\mathrm{I}}(x,s)=\frac{\beta_2 D_1+\Sigma_t}{\beta_2(D_1-D_2)}\exp(D_1 h) - \frac{\beta_2 D_2+\Sigma_t}{\beta_2(D_1-D_2)}\exp(D_2 h), \quad (43)$$

where

$$D_{1,2}\equiv[-b\pm(b^2-4c)^{\frac{1}{2}}]/2,$$
$$b\equiv\Sigma_t(1/\beta_2+1/\beta_1),$$
$$c\equiv(\Sigma_t^2-\Sigma_s^2)/\beta_1\beta_2.$$

Region II. In order to find N_D^{II} and N_i^{II}, the continuity of the current in the incident direction across the plane AC and the fact that the diffracted current density on the plane AB is zero are used; that is,

$$N_i^{\mathrm{I}}(0,s)=N_i^{\mathrm{II}}(0,s) \quad (44)$$

and

$$N_D^{\mathrm{II}}(x,0)=0. \quad (45)$$

Knowing that the solution for N_D must be of the form of Eq. (34), we find by applying these boundary conditions that

$$N_D^{\mathrm{II}}(x,s)=\exp[-\Sigma_t(x+s)] \times\sum_{n=1}^{\infty} A_{-n}^{\mathrm{II}}\left(\frac{s}{x}\right)^{n/2} I_n[2\Sigma_s(xs)^{\frac{1}{2}}] \quad (46)$$

and

$$N_i^{\mathrm{II}}(x,s)=\exp[-\Sigma_t(x+s)] \times\sum_{n=0}^{\infty} A_{-n-1}^{\mathrm{II}}\left(\frac{s}{x}\right)^{n/2} I_n[2\Sigma_s(xs)^{\frac{1}{2}}], \quad (47)$$

where

$$A_n^{\mathrm{II}}=\frac{(\beta_2 D_1+\Sigma_t)^{n+1}}{\Sigma_s{}^n\beta_2(D_1-D_2)}+\frac{(D_2\beta_2+\Sigma_t)^{n+1}}{\Sigma_s{}^n\beta_2(D_1-D_2)}. \quad (48)$$

Since the functions I_n are well tabulated, the diffracted current density leaving the crystal due to a finite incident beam can be easily calculated using Eqs. (42) and (46) and doing the subtraction indicated in Eq. (40). The series in (46) will be found to converge very rapidly when the thickness of the crystal T is of the order of $1/\Sigma_s$.

III. EXPERIMENTAL

We have performed experiments on the spatial distribution of the diffracted current from a variety of single-crystal slabs including Zn, NaCl, Pb, Cu, and Si. The results on the (000,2) reflection in a single Zn crystal with faces parallel to the basal planes of the hexagonal lattice are given here. The data obtained on the other crystals are similar to, and consistent with, the results on Zn.

In order to measure a spatial profile for a given value of Σ_s, $\mathbf{k}$ must be well defined since Σ_s depends very strongly on the orientation and magnitude of $\mathbf{k}$. This was accomplished by using the (111) reflection in a Si single crystal to produce a "monoenergetic" beam which was then collimated using two Cd slits with aperture 0.12 cm spaced 125 cm apart to give an angular resolution of about 4 min of arc.

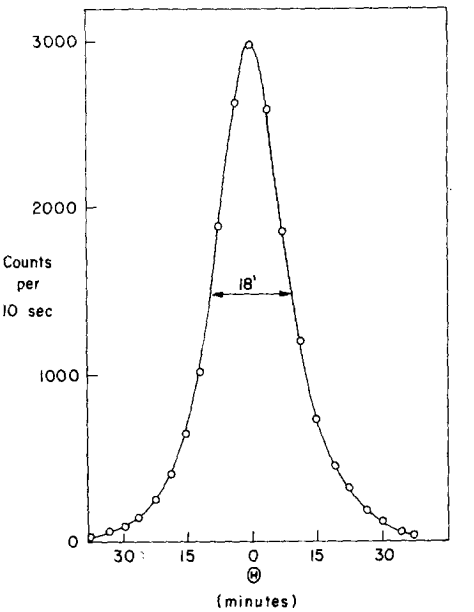

FIG. 10. Rocking curve for the (000,2) reflection in a Zn crystal. The incident beam is 0.12 cm wide with an angular spread of about 4 min of arc. The beam was monochromated with the Si (111) reflection to give a nominal wavelength of $\lambda=2.095$ Å.

A rocking curve for the Zn (000,2) reflection is shown in Fig. 10, the angular width of which is primarily due to the mosaic structure of the Zn crystal itself. Consequently, with the crystal fixed in angle at the peak counting rate, only those small-angle mosaic grains which are very close to the center of the mosaic distribution W are contributing to the reflection, and the value of Σ_s should be approximately[6]

$$\Sigma_s=[1/(2\pi)^{\frac{1}{2}}\eta]Q \quad (49)$$

under a Gaussian approximation to the mosaic distribution. η is the mosaic spread parameter and Q is given by

$$Q=(2\pi)^3|F|^2/V^2k^3\sin 2\theta_B, \quad (50)$$

where F = structure factor and V = volume of a unit cell. A first-order estimate of η can be obtained from the rocking curve by subtracting out the angular resolution of the incident beam.

In addition to the above method for calculating Σ_s, it can be obtained directly from the total current ratio.[6]

$$P_D/P_0=[1+(\beta_1/\Sigma_s T)]^{-1} \quad (51)$$

in the event that absorption and incoherent scattering are small compared to Σ_s (as is the case for Zn).

[6] See, for example, G. E. Bacon and R. D. Lowde, Acta Cryst. 1, 303 (1948).

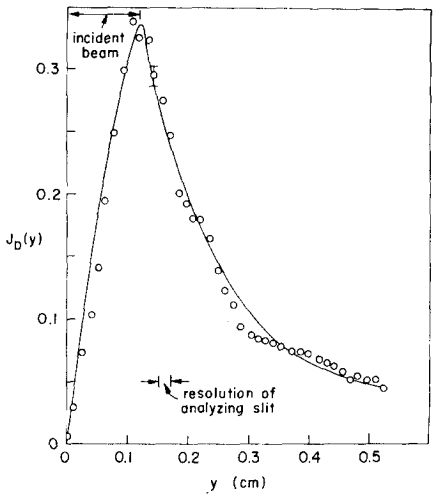

FIG. 11. Spatial distribution of the diffracted current density from a Zn crystal cut in the form of a slab with the (000,2) planes parallel to the surface. This distribution was taken with the crystal oriented at the peak of the rocking curve (Fig. 10). The crystal was rotated about the scattering vector to insure that there were no competing reflections. The crystal was 0.3 cm thick.

By moving a very narrow Cd slit across the diffracted beam when the crystal is fixed at its peak counting rate, the spatial distribution shown in Fig. 11 was obtained. The profile peaks at the "effective" right edge of the collimator and falls off gradually with a long "tail" as predicted in BRI and in Sec. II of this paper. The theoretical (solid) curve which fits the data reasonably well gives a value of $\Sigma_s = 3.0$ cm^{-1}. (The data were not normalized to the incident beam intensity in performing this fitting process.) Table I gives the values of Σ_s obtained from the three "independent" methods of measurement.

The discrepancy noted here between the various methods of measurement on Zn was also observed for the other crystals examined. The intensity of the diffracted beam is always less than expected. This gives the impression that there are certain orientation angles in the mosaic distribution for which there are no mosaic grains, hence neutrons of a particular **k** can pass undiminished. If there are, in fact, "holes" in the mosaic structure, they must be closely spaced. Otherwise they would be observed in double-crystal rocking curves using identical crystals, and they are not.

[The quality of our beam from this Si monochromator has been checked many times in several ways, and consequently normalization of the data to the incident beam should have led to compatible results. The contributions to the incident beam due to multiple reflections of $\frac{1}{2}\lambda$, $\frac{1}{3}\lambda$, $\frac{1}{4}\lambda$, $\frac{1}{5}\lambda$, and the epicadmium parts total less than $\frac{1}{2}\%$ of the first-order "pure" $\lambda = 2.095$-Å component. Scattering lengths obtained from various powder and polycrystalline samples agree very well with published cross-section data.]

TABLE I. Values of Σ_s from three methods of measurement.

		Σ_s[cm^{-1}]
(A)	From Eq. (49)	4.2
(B)	From Eq. (51)	0.702
(C)	Spatial distribution	3.0

IV. CONCLUSIONS

We feel that the discrepancies noted in Table I in the measurement of Σ_s are real and are related to the mosaic structures of crystals in general. There are many factors and parameters which can be varied easily in examining crystals by neutron diffraction in order to obtain a better understanding of the imperfections which occur naturally in all crystals. Varying the size and angular spread of the beam, the region of the crystal irradiated, and the incident energy are a few of these. The analysis given in this paper should be viewed simply as a starting point, providing certain guidelines for further study and experiments in this area. We emphasize again that the spatial distribution of the diffracted current density is of prime importance in this connection.

APPENDIX

Equations for calculating the coefficients a_l^n occurring in the calculations of Sec. II:

Even regions:

$$a_{-l}^{(2n)} = \sum_{m=0}^{\infty} [(\Sigma_s T/\beta_1)^m/m!] a_{m-l}^{(2n-1)}, \quad l \geq 1 \tag{A1}$$

$$a_0^{(2n)} = 0 \tag{A2}$$

$$a_l^{(2n)} = -\left(\frac{\beta_1}{\beta_2}\right)^l \sum_{m=0}^{\infty} [(\Sigma_s T/\beta_1)^m/m!] a_{m-l}^{(2n-1)}, \quad l \geq 1. \tag{A3}$$

Odd regions:

$$a_l^{(2n+1)} = \sum_{m=0}^{\infty} [(\Sigma_s T/\beta_2)^m/m!] a_{l-m}^{(2n)}, \quad l \geq 0 \tag{A4}$$

$$a_{-1}^{(2n+1)} = 1 \tag{A5}$$

$$a_{-l}^{(2n+1)} = (\beta_2/\beta_1)^{(l-1)/2}(c_0^{l-1} + c_0^{-l+1}) - (\beta_2/\beta_1)^{l-1} \sum_{m=0}^{\infty} [(\Sigma_s T/\beta_1)^m/m!] a_{l-m+2}^{(2n)}, \quad l \geq 2, \tag{A6}$$

where

$$c_0 = c_1 + (c_1^2 - 1)^{\frac{1}{2}} \tag{A7}$$

$$c_1 = \tfrac{1}{2}(\Sigma_t/\Sigma_s)[(\beta_1/\beta_2)^{\frac{1}{2}} + (\beta_2/\beta_1)^{\frac{1}{2}}]. \tag{A8}$$